Effects of dense matter properties on the tidal deformability and gravitational waveforms of binary neutron stars

L. Perot and N. Chamel

Institut d'Astronomie et d'Astrophysique, CP-226, Université Libre de Bruxelles, 1050 Brussels, Belgium

Abstract

The role of the dense matter properties on the tidal deformability and gravitational waveforms of binary neutron stars is studied using a set of unified equations of state. Based on the nuclear energy-density functional theory, these equations of state provide a thermodynamically consistent treatment of all regions of the stars and were calculated using functionals that were precision fitted to experimental and theoretical nuclear data.

I Introduction

Formed in gravitational core-collapse supernova explosions, neutron stars are the most compact stars in the Universe. Their average density exceeds than that found in atomic nuclei. **The interior of a neutron star exhibits very different phases of matter** (see, e.g. Ref. [1] for a recent review):

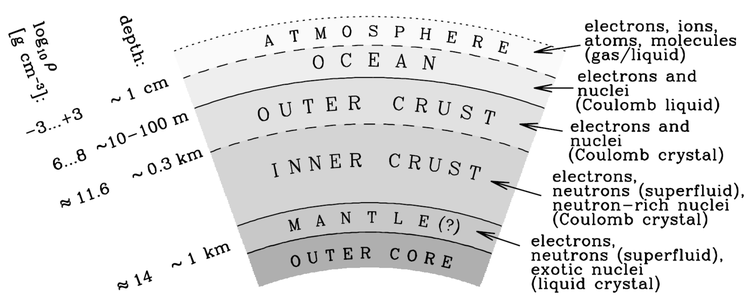

Taken from P. Haensel, A. Y. Potekhin, D. G. Yakovlev, *Neutron Stars* (Springer, 2007).

II Nuclear energy density functional theory

In the nuclear energy-density functional (EDF) theory [2], nucleons are treated as independent quasiparticles in self-consistent potentials via the Hartree-Fock-Bogolyubov (HFB) method. A family of EDFs [3, 4] were recently constructed, all based on extended Skyrme effective nucleon-nucleon interactions [5] and **precision-fitted to essentially all experimental atomic mass data with a rms deviation as low as 0.5-0.6 MeV**.

To assess the role of nuclear uncertainties, the series BSk19- BSk21 were simultaneously fitted to different realistic neutron-matter equations of state (EoS) with different degrees of stiffness, while the series BSk22-BSk25 mainly differ in their predictions for the symmetry energy (BSk26 being fitted to the same symmetry-energy coefficient at saturation as BSk24 but to a different neutron-matter EoS).

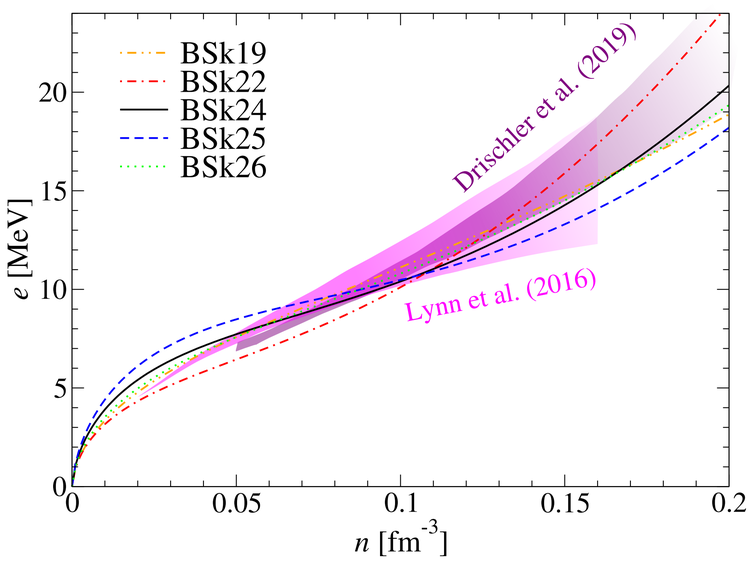

Variations of the energy per particle in neutron matter with density n. The shaded areas represent constraints obtained from chiral effective field theory [6, 7]. Results for BSk20 and BSk21 are indistinguishable from those obtained for BSk26 and BSk24, respectively.

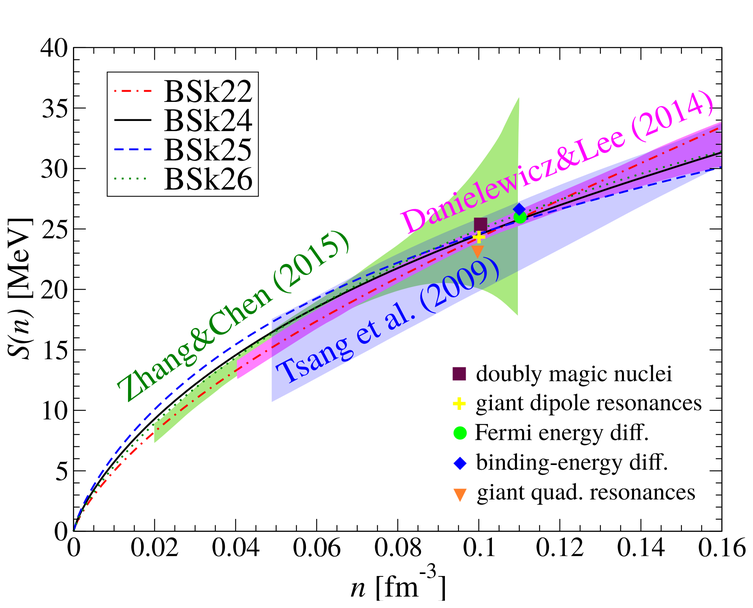

Variation of the symmetry energy $S(n)$ with density n. The shaded areas are experimental constraints: from heavy-ion collisions [8] (blue), from isobaric-analog states and neutron skins [9] (purple), and from the electric dipole polarizability of ^{208}Pb [10] (green). Results for BSk20 and BSk21 are indistinguishable from those obtained for BSk26 and BSk24, respectively.

These EDFs are well suited for applications to neutron stars.

III Equations of state of dense matter

The interior of a neutron star is supposed to be cold and fully 'catalyzed'. A detailed account of the calculations in the different regions of a neutron star can be found in Ref. [11]. The equilibrium properties of the outer crust for densities $\rho \gtrsim 10^6$ g cm^{-3} were determined using experimental atomic mass data supplemented by HFB masses. For the inner crust, the 4th-order extended Thomas-Fermi method was adopted within the Wigner-Seitz approximation using parametrised nucleon distributions. Proton shell and pairing corrections were added perturbatively. Calculations in the core are comparatively much simpler since the EoS is given by analytic expressions. **Complete numerical results and fits applicable to the entire star** can be found in Refs. [11, 12].

IV Tidal deformability of neutron stars

In a binary system, each neutron star is deformed due to tidal forces. The tidal field can be decomposed into an "electric" component $\mathcal{E}_L$, where L denotes a set of space indices $i_1 i_2 \cdots i_\ell$, and a "magnetic" component $\mathcal{M}_L$ (which is absent in Newtonian theory), inducing inside the star a mass multipole moment $\mathcal{Q}_L$ and a current multipole moment $\mathcal{S}_L$ respectively. To leading order, these induced moments are given by

$$\mathcal{Q}_L = \lambda_\ell \mathcal{E}_L \,,$$
$$\mathcal{S}_L = \sigma_\ell \mathcal{M}_L \,,$$

where the coefficients λ_ℓ and σ_ℓ are respectively referred to as the gravitoelectric and gravitomagnetic tidal deformabilities of order ℓ, and are related to the corresponding dimensionless tidal Love numbers through:

$$k_\ell = \frac{1}{2}(2\ell-1)!! \frac{G\lambda_\ell}{R^{2\ell+1}} \,,$$
$$j_\ell = 4(2\ell-1)!! \frac{G\sigma_\ell}{R^{2\ell+1}} \,,$$

where R denotes the circumferential radius of the star and G is the gravitational constant. **The radius R and the Love numbers k_ℓ and j_ℓ depend on the dense-matter EoS.** The detailed formalism to calculate Love numbers can be found in Ref. [14].

Most previous studies focused on the $\ell = 2$ Love numbers (see, e.g., Ref. [13]). We have recently calculated tidal deformabilities up to $\ell = 5$. We show here results for $\ell = 3$:

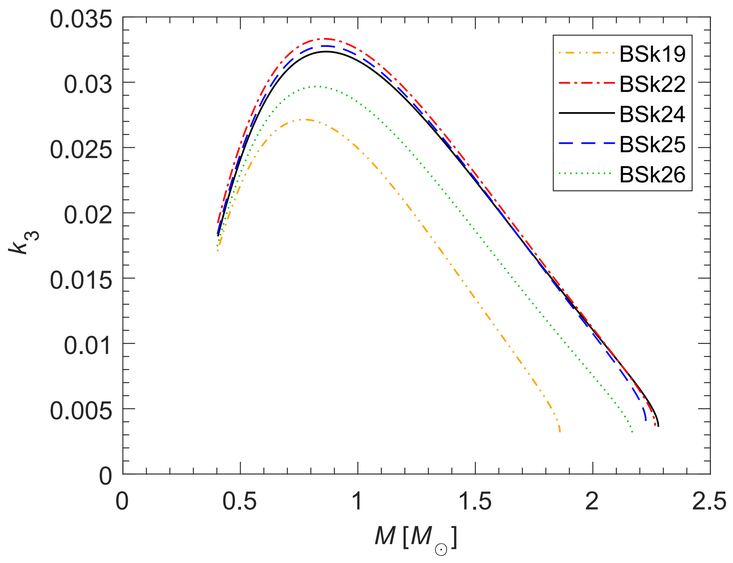

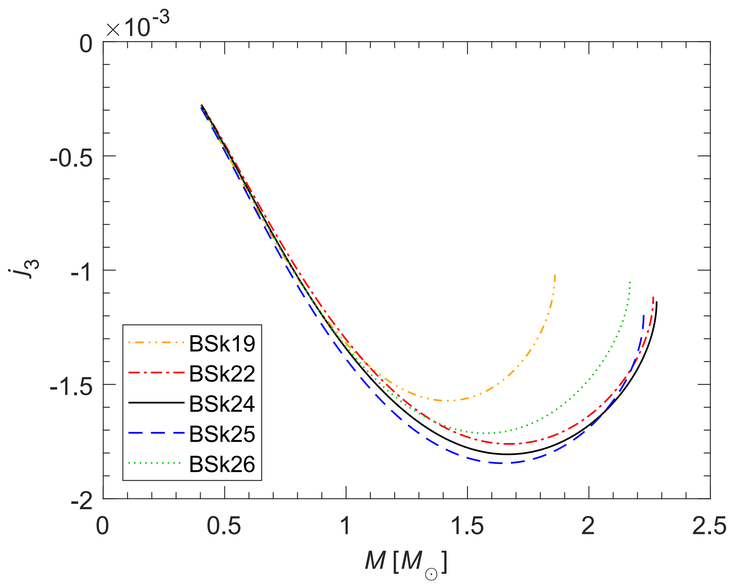

Comparing results for BSk22, BSk24 and BSk25 shows that the symmetry energy plays a minor role both for k_3 and j_3 (calculated here for an irrotational fluid, which is more realistic than a purely static fluid). **The key factor appears to be the stiffness of the neutron-matter EoS**, as can be clearly seen by comparing results for BSk19, BSk26, and BSk24 (by increasing order of stiffness): the softer the EoS is, the lower is the value for k_3 and j_3 (in absolute value) for a given neutron star mass. The hierarchy between the different EoS curves for higher ℓ remains the same; however, the impact of the symmetry energy on k_ℓ becomes more visible with increasing ℓ, contrary to j_ℓ. The full results up to $\ell = 5$ are displayed in Ref. [14].

The magnitude of both the gravitoelectric and gravitomagnetic Love numbers decreases with increasing ℓ. For a $1.4M_\odot$ neutron star with the BSk24 EoS, the values of k_5 and j_5 represent only 4% and 3% of those of k_2 and j_2, respectively.

V Impact on the gravitational-wave phase

We show here the tidal corrections to the gravitational-wave (GW) phase Ψ_2 and $\widetilde{\Psi}_2$ respectively associated with the gravitoelectric and gravitomagnetic Love numbers k_2 and j_2 (for an irrotational fluid), as a function of the frequency f and considering binary systems with both neutron stars having a mass $M = 1.4M_\odot$. Because the post-newtonian approximation breaks down near the merger, the phases are only plotted up to $f = 1000$ Hz:

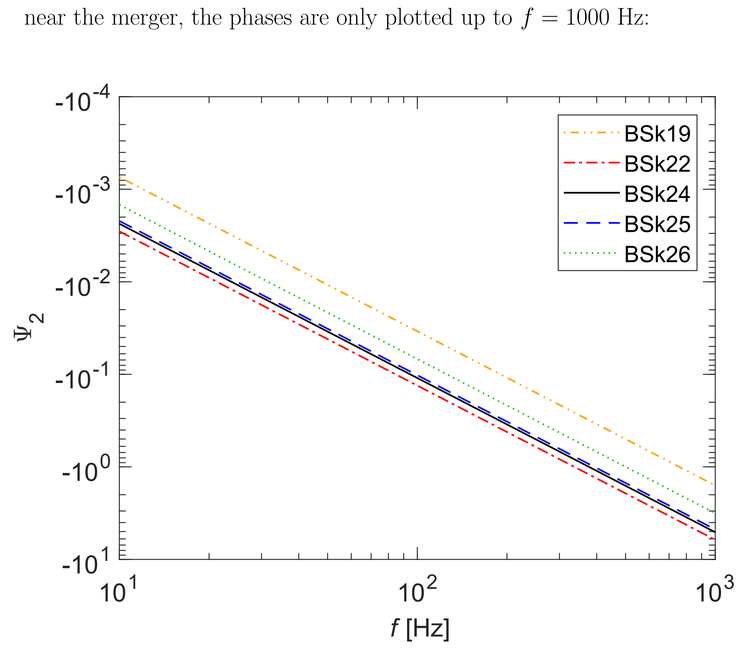

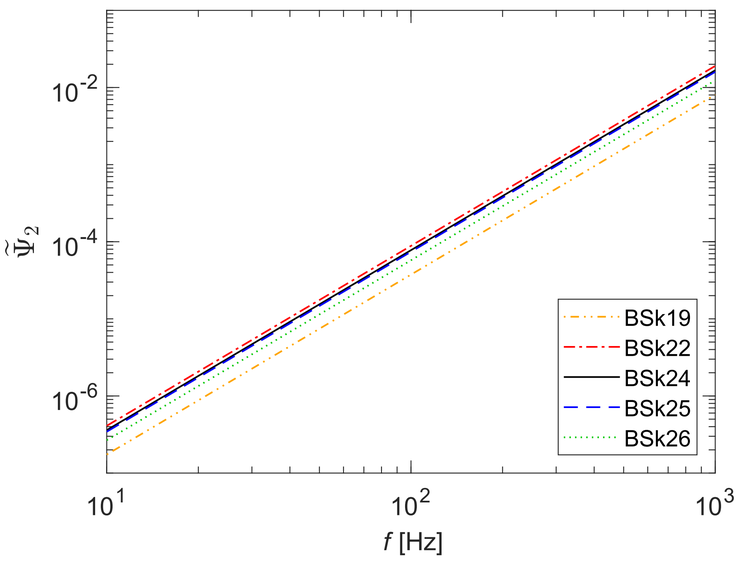

Extracting information about the symmetry energy from the GW signal during the inspiral phase will be very difficult, as can be seen by comparing results obtained for BSk22, BSk24, and BSk25. On the other hand, the stiffness of the neutron-matter EoS leaves a clear imprint on the waveform. The comparison of the results obtained for BSk19, BSk26 and BSk24 shows that **the softer the EoS is, the more pronounced are the tidal effects.**

The relative importance of the different ℓ-terms is found to follow the same hierarchy as the Love numbers. In particular, the tidal correction Ψ_3 associated with k_3 is about two orders of magnitude smaller than the leading tidal term Ψ_2. The correction $\widetilde{\Psi}_2$ induced by j_2 lies between those associated with k_3 and k_4. For detailed results, see Ref. [14].

VI Conclusions

The role of the dense matter properties on the tidal deformability and gravitational waveforms of binary neutron stars has been studied using the series of unified EoSs BSk19-26 all based on the nuclear EDF theory. For these EoSs, we have shown that the symmetry energy has essentially no impact on both gravitoelectric and gravitomagnetic Love numbers, characterizing the tidal response of neutron stars; the key factor appears to be the stiffness. In the same way, we have shown that the tidal phase correction to the GW signal also depend mostly on the stiffness: the softer the EoS is, the more pronounced are the tidal effects.

Acknowledgments

This work was supported by Fonds de la Recherche Scientifique - FNRS (Belgium) under grant No. 1.B.410.18F. L. Perot is a FRIA grantee of the Fonds de la Recherche Scientifique.

References

[1] D. Blaschke and N. Chamel, in Astrophysics and Space Science Library, edited by L. Rezzolla, P. Pizzochero, D. I. Jones, N. Rea, and I. Vidana, Astrophysics and Space Science Library Vol. **457** (Springer, Berlin, 2018) p. 337-400.

[2] M. Bender, P.-H. Heenen and P.-G. Reinhard, Rev. Mod. Phys.**75**, 121 (2003).

[3] S. Goriely, N. Chamel, and J. M. Pearson, Phys. Rev. C **82**, 035804 (2010).

[4] S. Goriely, N. Chamel, and J. M. Pearson, Phys. Rev. C **88**, 024308 (2013).

[5] N. Chamel, S. Goriely, and J. M. Pearson, Phys. Rev. C **80**, 065804 (2009).

[6] J. E. Lynn et al., Phys. Rev. Lett. **116**, 062501 (2016).

[7] C. Drischler, K. Hebeler, and A. Schwenk, Phys. Rev. Lett. **122**, 042501 (2019).

[8] M. B. Tsang et al., Phys. Rev. Lett. **102**, 122701 (2009).

[9] P. Danielewicz and J. Lee, Nucl. Phys. **A 922**, 1 (2014).

[10] Z. Zhang and L.-W. Chen, Phys. Rev. C **92**, 031301(R) (2015).

[11] J. M. Pearson et al., MNRAS **481**, 2994 (2018).

[12] A. Y. Potekhin et al., A&A **560**, A48 (2013).

[13] L. Perot, N. Chamel, A. Sourie, Phys. Rev. C **100**, 035801 (2019).

[14] L. Perot, N. Chamel, Phys. Rev. C **103**, 025801 (2021).